Compressed Sensing in MIMO Radar

Chun-Yang Chen and P. P. Vaidyanathan
Dept. of Electrical Engineering, MC 136-93
California Institute of Technology, Pasadena, CA 91125, USA
E-mail: cyc@caltech.edu, ppvnath@systems.caltech.edu

***Abstract*—Compressed sensing is a technique for efficiently sampling signals which are sparse in some transform domain. Recently, the idea of compressed sensing has been used in the radar system. When the number of targets on the range-Doppler plane is small, the target scene can be reconstructed by employing the compressed sensing techniques. In this paper, we extend this idea to the MIMO radar. In the MIMO radar, the compressed sensing technique can be used to reconstruct the target scene when the signals are sparse in the range-Doppler-angle space. To effectively reconstruct the target scene, it is required that the correlation between the target responses be small. In this paper, a waveform design method is introduced to reduce the correlations between target responses. Because of the increased dimensionality in MIMO radars as compared to phased array radars, the impact of compressed sensing will be very significant there.** [1]

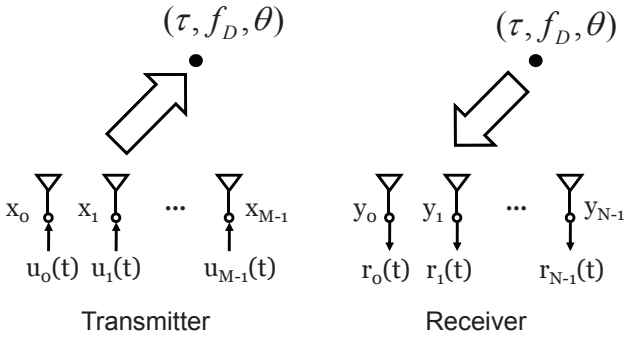

Fig. 1. Illustration of the MIMO radar transmitter and receiver.

I. Introduction and Signal Model

The idea of using compressed sensing in radar receiver was introduced by Herman and Strohmer in [1]. It is demonstrated in [1] that when the target scene is sparse in range-Doppler plane, the compressed sensing can be very effective. In this paper, we extend their work to the MIMO radar case. In the MIMO radar case, the parameter space contains not only delay and Doppler but also the angle. Because of the new angle dimension introduced by the MIMO radar, the sparsity of target scene is easier to obtain. The sparsity is essential for the compressed sensing recovery. Therefore the impact of compressed sensing in MIMO radar will be more significant.

Consider a MIMO radar consisting of a linear transmitting antenna array with M elements and a linear receiving antenna array with N elements. The transmitting antennas are located in the positions $\frac{\lambda}{2} \cdot (x_0, x_1, \cdots, x_{M-1})$ and the receiving antennas are located in $\frac{\lambda}{2} \cdot (y_0, y_1, \cdots, y_{N-1})$, where λ is the wavelength. Fig. 1 illustrates such a system. The mth transmitting antenna emits the signal $u_m(t)e^{j2\pi f_c t}$, where f_c is the carrier frequency. The nth receiving antenna receives the signal $r_n(t)e^{j2\pi f_c t}$. When there is only one point target with Doppler frequency f_D, delay τ, and angle θ, the received signal can be expressed as

$$r_n(t) \propto \sum_{m=0}^{M-1} u_m(t-\tau)e^{j2\pi f_D t}e^{j\pi \sin\theta(x_n+y_m)},$$

for $n = 0, 1, \cdots, N-1$. Our goal is to detect the target and estimate its radar cross section (RCS) from the above received waveforms.

[1]Work supported in parts by the ONR grant N00014-08-1-0709 and the California Institute of Technology.

II. Compressed Sensing in MIMO Radar Receiver

In order to use the compressed sensing recovery techniques, we need to sample the received signal $r_n(t)$. Define

$$\mathbf{r}_n = (r_n(0), r_n(T_s), \cdots, r_n((K-1)T_s))^T,$$

for $n = 0, 1, \cdots, N-1$, and

$$\mathbf{u}_m = (u_m(0), u_m(T_s), \cdots, u_m((L-1)T_s))^T,$$

for $m = 0, 1, \cdots, M-1$, where T_s is the sampling period and L and K are the numbers of samples in the transmitted waveform and received waveform respectively, where we choose $K \geq 2L$. The sampled received signal can be represented as

$$\mathbf{r}_n \propto \sum_{m=0}^{M-1} \mathbf{C}_{\alpha_\tau}\mathbf{D}_{\alpha_D}\mathbf{u}_m e^{j\frac{\alpha_\theta}{N_\theta}(x_m+y_n)},$$

for $n = 0, 1, \cdots, N-1$, where

$$\mathbf{C}_{\alpha_\tau} = \begin{pmatrix} \mathbf{0}_{\alpha_\tau \times L} \\ \mathbf{I}_L \\ \mathbf{0} \end{pmatrix},$$

$$\mathbf{D}_{\alpha_D} \triangleq \text{diag}\{1, e^{j2\pi\frac{\alpha_D}{N_D}}, \cdots, e^{j2\pi\frac{\alpha_D}{N_D}(L-1)}\},$$

N_D is the resolution of the Doppler frequency, N_θ is the resolution of the angle, $\alpha_\tau = 0, 1, \cdots, L-1$ represents the delay, $\alpha_D = 0, 1, \cdots, N_D - 1$ represents the Doppler shift, and $\alpha_\theta = 0, 1, \cdots, N_\theta - 1$ represents the angle. Define

$$\mathbf{r} = (\mathbf{r}_0^T, \mathbf{r}_1^T, \cdots, \mathbf{r}_{N-1}^T)^T,$$
$$\mathbf{u} = (\mathbf{u}_0^T, \mathbf{u}_1^T, \cdots, \mathbf{u}_{M-1}^T)^T, \text{ and}$$
$$(\mathbf{A}_{\alpha_\theta})_{n,m} = e^{j\alpha_\theta(x_m+y_n)},$$

for $n = 0, 1, \cdots, N-1$ and $m = 0, 1, \cdots, M-1$. The overall input-output relation can be represented as

$$\mathbf{r} \propto \underbrace{\mathbf{A}_{\alpha_\theta} \otimes \mathbf{C}_{\alpha_\tau} \mathbf{D}_{\alpha_D}}_{\mathbf{H}_{\boldsymbol{\alpha}}} \cdot \mathbf{u}.$$

To simplify the notation, we further define

$$\mathbf{H}_{\boldsymbol{\alpha}} = \mathbf{A}_{\alpha_\theta} \otimes \mathbf{C}_{\alpha_\tau} \mathbf{D}_{\alpha_D},$$

where $\boldsymbol{\alpha} \triangleq (\alpha_\theta, \alpha_\tau, \alpha_D)$. When there are multiple targets, the received signal can be expressed as

$$\mathbf{r} = \left(\sum_{\boldsymbol{\alpha}} s_{\boldsymbol{\alpha}} \mathbf{H}_{\boldsymbol{\alpha}} \right) \cdot \mathbf{u},$$

where the scalar $s_{\boldsymbol{\alpha}}$ represents the radar cross section (RCS) of the target in the $\boldsymbol{\alpha}$th range-Doppler-angle cell as shown in Fig. 2. The input-output relation is illustrated in Fig. 3. Defining

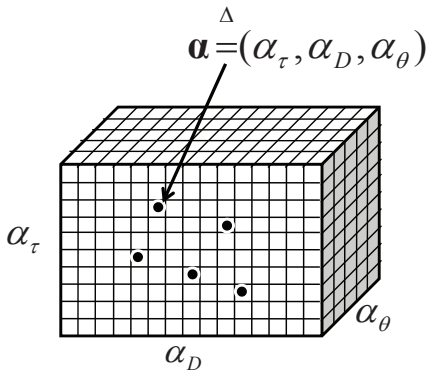

Fig. 2. Illustration of range-Doppler-angle space.

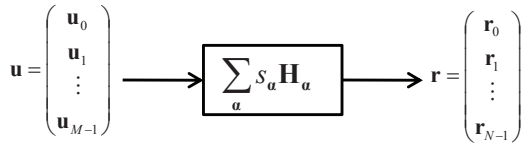

Fig. 3. Illustration of input-output relation.

$\mathbf{b}_{\boldsymbol{\alpha}} = \mathbf{H}_{\boldsymbol{\alpha}} \cdot \mathbf{u}$, the input-output relation can be rewritten as

$$\mathbf{r} = \sum_{\boldsymbol{\alpha}} s_{\boldsymbol{\alpha}} \mathbf{b}_{\boldsymbol{\alpha}} = \boldsymbol{\Phi} \mathbf{s}, \tag{1}$$

where $\boldsymbol{\Phi}$ is a matrix consisting of column vectors $\{\mathbf{b}_{\boldsymbol{\alpha}}\}$ and $\mathbf{s}$ is a $KN_DN_\theta \times 1$ vector consisting of elements $\{s_{\boldsymbol{\alpha}}\}$. Our goal is to detect the targets and to estimate their RCS. In other words, we want to solve for the vector $\mathbf{s}$ in the above equation. Solving for $\mathbf{s}$ in (1) can be viewed as an ordinary inverse problem. Least square method is a well-known powerful tool for solving this type of problems. However, if the target scene $\mathbf{s}$ is known to be sparse (i.e. $\left|\{\boldsymbol{\alpha} \mid s_{\boldsymbol{\alpha}} \neq 0\}\right| \ll KN_DN_\theta$), then compressed sensing techniques will give a much better performance than the least square method. Compressed sensing reconstruction algorithms such as basis pursuit [2], matching pursuit [3], and orthogonal matching pursuit [4] are well-known for solving this type of problems. In [1], the compressed sensing reconstruction algorithms have been applied for reconstructing the target scene in a single-input single-output radar system. In this paper we apply these methods in the MIMO radar to reconstruct the sparse target scene vector $\mathbf{s}$ in (1). The numerical example of the recovery results will be shown in Sec. IV. It shows that the compressed sensing based receiver has a better performance than the matched filter based approaches.

III. Waveform Optimization

To obtain good reconstruction by the compressed sensing techniques, it has been shown that the coherence of the matrix $\boldsymbol{\Phi}$ must be sufficiently small [5], where the coherence has been defined as

$$\begin{aligned} \mu(\mathbf{u}) &\triangleq \max_{\boldsymbol{\alpha} \neq \boldsymbol{\alpha}'} | < \mathbf{b}_{\boldsymbol{\alpha}}, \mathbf{b}_{\boldsymbol{\alpha}'} > | \\ &= \max_{\boldsymbol{\alpha} \neq \boldsymbol{\alpha}'} | < \mathbf{H}_{\boldsymbol{\alpha}} \mathbf{u}, \mathbf{H}_{\boldsymbol{\alpha}'} \mathbf{u} > |. \end{aligned} \tag{2}$$

Therefore, we can choose the transmitted waveforms $\mathbf{u}$ so that the coherence $\mu(\mathbf{u})$ is reduced. Using the expression $\mathbf{H}_{\boldsymbol{\alpha}} = \mathbf{A}_{\alpha_\theta} \otimes \mathbf{C}_{\alpha_\tau} \mathbf{D}_{\alpha_D}$ and the property of Kronecker products, the correlation can be simplified as

$$\begin{aligned} < \mathbf{b}_{\boldsymbol{\alpha}}, \mathbf{b}_{\boldsymbol{\alpha}'} > &= \mathbf{u}^\dagger \mathbf{H}_{\boldsymbol{\alpha}'}^\dagger \mathbf{H}_{\boldsymbol{\alpha}} \mathbf{u} \\ &= \mathbf{u}^\dagger \left(\mathbf{A}_{\alpha'_\theta}^\dagger \mathbf{A}_{\alpha_\theta} \otimes \mathbf{D}_{\alpha'_D}^\dagger \mathbf{C}_{\alpha'_\tau}^\dagger \mathbf{C}_{\alpha_\tau} \mathbf{D}_{\alpha_D} \right) \mathbf{u} \\ &= \mathbf{u}^\dagger \left(\mathbf{A}_{\alpha'_\theta}^\dagger \mathbf{A}_{\alpha_\theta} \otimes \mathbf{Z}^{\alpha_\tau - \alpha'_\tau} \mathbf{D}_{\alpha_D - \alpha'_D} \right) \mathbf{u} \\ &\triangleq \kappa(\alpha'_\theta, \alpha_\theta, \alpha_\tau - \alpha'_\tau, \alpha_D - \alpha'_D), \end{aligned}$$

where

$$\mathbf{Z} \triangleq \begin{pmatrix} 0 & 0 & \cdots & & 0 \\ 1 & 0 & 0 & \cdots & 0 \\ 0 & 1 & 0 & \ddots & \\ \vdots & \ddots & \ddots & \ddots & 0 \\ 0 & \cdots & 0 & 1 & 0 \end{pmatrix}.$$

One can observe that the correlation function can be expressed as a function of $\alpha_\tau - \alpha'_\tau$ and $\alpha_D - \alpha'_D$. The coherence of the matrix $\boldsymbol{\Phi}$ can thus be rewritten as

$$\mu(\mathbf{u}) = \max_{(\alpha_\theta, \Delta\alpha_\tau, \Delta\alpha_D) \neq (\alpha'_\theta, 0, 0)} |\kappa(\alpha_\theta, \alpha'_\theta, \Delta\alpha_\tau, \Delta\alpha_D)|. \tag{3}$$

By expressing the correlation in the form of (3) rather than (2), one can reduce the number of parameters from six to four. The reduction of the dimensions will greatly improve the performance of the waveform optimization algorithm which will be proposed later in this section.

Besides affecting the coherence of the matrix $\boldsymbol{\Phi}$, the choice of the waveform $\mathbf{u}$ will also affect the beamforming. Therefore we should also design the waveform such that it properly illuminate the angle of interest. The energy illuminating outside the angle of interest can be expressed as

$$\eta(\mathbf{u}) \triangleq \sum_{\alpha_\theta \notin \mathcal{A}} \kappa(\alpha_\theta, \alpha_\theta, 0, 0), \tag{4}$$

where $\mathcal{A}$ is the set consisting of angle of interest. By minimizing the above term, we can direct the energy to the angle of

interest. The flatness of the passband of the transmitted beam can be evaluate by the following term:

$$\zeta(\mathbf{u}) \triangleq \sum_{\alpha_\theta \in \mathcal{A}} \left| \kappa(\alpha_\theta, \alpha_\theta, 0, 0) - \frac{1}{|\mathcal{A}|} \sum_{\alpha_\theta \in \mathcal{A}} \kappa(\alpha_\theta, \alpha_\theta, 0, 0) \right|^2. \tag{5}$$

One can minimize the above term to make the transmit beam evenly illuminates the angle of interest.

In this paper, we consider phase hopping signals. The lth element of the mth transmitted waveform can be expressed as

$$u_m(l) = e^{j\frac{2\pi}{Q}c_{m,l}},$$

where $c_{m,l} \in \{0, 1, 2, \cdots, Q-1\}$ is the hopping code and Q is the number of hopping frequencies. The phase hopping signals are easy to generate and have the advantage of constant modulus. Combining all the cost functions from (3), (4) and (5), we define the following overall cost function:

$$f(\mathbf{C}) = \beta \cdot \mu(\mathbf{u}) + \gamma \cdot \eta(\mathbf{u}) + (1 - \beta - \gamma) \cdot \zeta(\mathbf{u}),$$

where $\mathbf{C}$ is a $M \times L$ matrix consisting of elements $\{c_{m,l}\}$, $u_m(l) = e^{j\frac{2\pi}{Q}c_{m,l}}$, and β and γ are the scalars which we can adjust to modify the cost function to emphasize the coherence, stopband energy, or passband flatness. The corresponding optimization problem can be expressed as

$$\begin{aligned} &\min_{\mathbf{C}} f(\mathbf{C}) \\ &\text{subject to} \quad \mathbf{C} \in \{0, 1, \cdots, Q-1\}^{ML} \end{aligned} \tag{6}$$

The feasible set of this problem is a discrete set. It is known that the simulated annealing algorithm [7] is a powerful tool for searching a suboptimal solution for this type of problems. In this paper, we use a simulated annealing algorithm to solve for the optimal phase hopping codes.

The simulated annealing algorithm runs a Markov chain Monte Carlo (MCMC) sampling on the discrete feasible set [8]. The transition probability of the Markov chain can be chosen so that the equilibrium of the Markov chain is

$$\begin{aligned} \pi_T(\mathbf{C}) &= \frac{1}{Z_T} \exp(\frac{-f(\mathbf{C})}{T}), \text{ where} \\ Z_T &= \sum_{\mathbf{C}} \exp(\frac{-f(\mathbf{C})}{T}). \end{aligned} \tag{7}$$

Here T is a parameter called temperature. By running the MCMC and gradually decreasing the temperature T, the generated sample $\mathbf{C}$ will have a high probability to have a small cost function output [7]. In our case, the transition probability from state $\mathbf{C}$ to $\mathbf{C}'$ is chosen as

$$p(\mathbf{C}, \mathbf{C}') = \begin{cases} \frac{1}{d}\min(1, \exp(\frac{f(\mathbf{C})-f(\mathbf{C}')}{T})), & \text{if } \mathbf{C}' \sim \mathbf{C} \\ 1 - \frac{1}{d}\sum_{\mathbf{C}'' \sim \mathbf{C}} \min(1, \exp(\frac{f(\mathbf{C})-f(\mathbf{C}'')}{T})), & \text{if } \mathbf{C}' = \mathbf{C} \\ 0, & \text{otherwise,} \end{cases}$$

where $\mathbf{C}' \sim \mathbf{C}$ denotes that $\mathbf{C}'$ and $\mathbf{C}$ differ in exactly one element, and d denotes $\left|\{\mathbf{C}' \middle| \mathbf{C}' \sim \mathbf{C}\}\right|$. It can be shown that the chosen transition probabilities result in the desire equilibrium in (7) [8]. The numerical results of this algorithm are shown in the next section.

IV. Numerical Results

In this section, the following parameters are used:

1) the number of transmitting antennas $M = 4$,
2) the number of receiving antennas $N = 10$,
3) the transmitting antenna location $x_m = N \cdot m$, for $m = 0, 1, \cdots, M-1$,
4) the receiving antenna location $y_n = n$, for $n = 0, 1, \cdots, N-1$,
5) the length of the transmitted waveform $L = 31$,
6) the number of hopping frequencies $Q = 31$,
7) the resolution of the angle $N_\theta = 40$,
8) the resolution of the Doppler shift $N_D = 1$,
9) and the desired beampattern is omnidirectional.

Fig. 4 shows the histogram of all the correlations $\{|\kappa(\alpha_\theta, \alpha'_\theta, \Delta\alpha_\tau, \Delta\alpha_\theta)\}$. We compare the signal generated

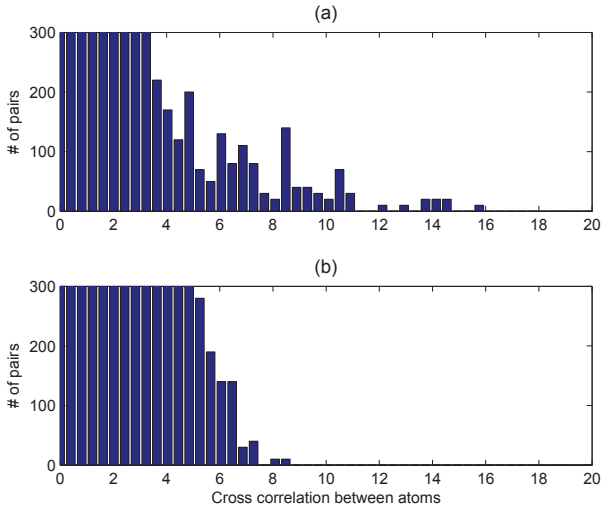

Fig. 4. Histogram of the correlations between the target responses: (a) Alltop sequence [1] and (b) The proposed method.

by the proposed algorithm and the Alltop sequence used in [1]. According to [1], the Alltop sequence has a nearly optimal coherence in the phased array radar case. However, in the MIMO radar case, one can see that the proposed algorithm generates the waveform with smaller target response correlation compared to the Alltop sequence.

Fig. 5 shows the example of the target scene reconstruction. Fig. 5 (a) shows the original target scene and the corresponding vector $\mathbf{s}$. Fig 5 (b) shows the target scene reconstructed by the compressed sensing recovering method. Here we use the method of orthogonal matching pursuit [4]. Fig 5 (c) shows the target scene reconstructed by the matched filtering. Fig 5 (d) shows the target scene reconstructed by the matched filtering and thresholding. In all three cases, the waveform obtained by the proposed algorithm is transmitted and the noise in the receiver is additive 0dB white noise. One can see that the compressed sensing algorithm obtains a much better recovery than the matched filtering based approaches.

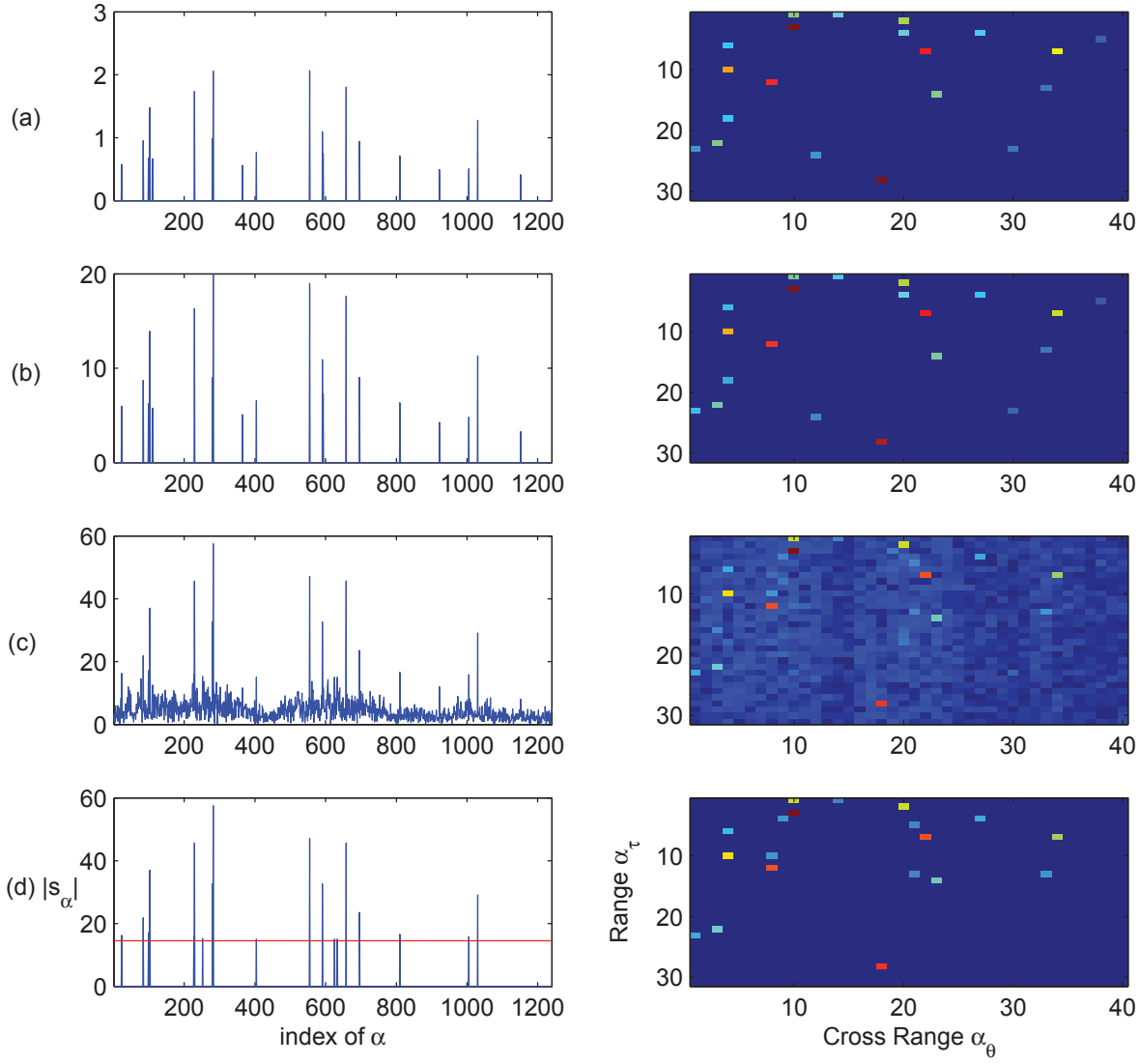

Fig. 5. Comparison of the reconstructed target scene: (a) Original target scene, (b) Target scene reconstructed by compressed sensing, (c) Target scene reconstructed by matched filtering, and (d) Target scene reconstructed by matched filtering with thresholding

V. Conclusions

In this paper, we have extended the idea of using compressed sensing recovery in radar to the MIMO radar case. The corresponding waveform optimization method has also been proposed. Numerical results show that the compressed sensing method has a better performance than the matched filter approach when the target scene is sparse.

References

[1] M. Herman and T. Strohmer, "Compressed Sensing Radar," *Proc. IEEE Int. Conf. Acoust., Speech Sig. Proc.,* Mar 2008.

[2] S. S. Chen, D. L. Donoho, and M. A. Saunders, "Atomic decomposition by basis pursuit," *SIAM J. Sci. Comput.,* vol. 20, no. 1, pp. 33-61, 1999.

[3] S. Mallat and Z. Zhang, "Matching pursuits with time-frequency dictionaries," *IEEE Trans. Signal Processing,* vol. 41, pp. 3397-3415, Dec. 1993.

[4] S. Chen, S. A. Billings, and W. Luo, "Orthogoanl least squres methods and their application to nonlinear system identification," *Intl. J. Contr.* vol. 50, no. 5, pp. 1873-1896, 1989.

[5] J. A. Tropp, "Greed is Good: Algorithmic Results for Sparse Approximation," *IEEE Transactions on Information Theory,* Vol. 50, Issue. 10, Oct. 2004.

[6] E. J. Candes and T. Tao, "Decoding by Linear Programming," *IEEE Transactions on Information Theory,* Vol. 51, Issue. 10, Dec. 2005.

[7] S. Kirkpatrick, C. D. Gelatt and M. P. Vecchi, "Optimization by Simulated Annealing," *Science,* Vol. 220, no. 4598, pp. 671-680, 1983.

[8] N. Metropolis, A.W. Rosenbluth, M.N. Rosenbluth, A.H. Teller, and E. Teller. "Equations of State Calculations by Fast Computing Machines," Journal of Chemical Physics, Vol. 21, no. 6, pp. 1087-1092, 1953.